Research Square

Preprints are preliminary reports that have not undergone peer review.
They should not be considered conclusive, used to inform clinical practice,
or referenced by the media as validated information.

Morphogenesis of the Drosophila antennal auditory structure in the pupa, with a focus on the connection between the sensory organ and the exoskeleton

Shan Jiang
Chiba University
Reiko Tajiri
rtajiri@chiba-u.jp

Chiba University

Research Article

Keywords:

Posted Date: June 24th, 2026

DOI: https://doi.org/10.21203/rs.3.rs-10001040/v1

License: This work is licensed under a Creative Commons Attribution 4.0 International License.
Read Full License

Additional Declarations: No competing interests reported.

Version of Record: A version of this preprint was published at Discover Developmental Biology on October 2nd, 2026. See the published version at https://doi.org/10.1007/s00427-026-00734-2.

Abstract

Hearing is an important physiological function for animals to perceive their external environment and to communicate with each other. For example, *Drosophila* females use their antennae to recognize species-specific courtship songs produced by males. In *Drosophila*, sounds are detected the Johnston's Organs (JO), an array of mechanoreceptors located in the second antennal segment (a2). Sounds cause vibration of the distal (third) antennal segment (a3), which in turn causes rotation of the a2-a3 joint exoskeleton, to which the JO is connected. The a2-a3 joint exhibits an elaborate structure, and mutations that disrupt the structure are associated with hearing defects. How the elaborate joint structure and its connection to JO develop remains to be understood. Here we show their morphogenetic processes during the pupal stage, with focus on the a2-a3 joint and JO. We first describe invagination of the epidermis at the a2-a3 joint prior to cuticle formation. Then we clarify how the cellular and extracellular structures of the JO that mediate its attachment to the a2-a3 joint exoskeleton (epidermis/cuticle) develop. We further searched for genes that were expressed in the a2-a3 joint epidermis, as a step toward exploring the genetic pathway regulating the JO-exoskeleton connection. We found that an enhancer trap of *big brain* (*bib*), a target gene of Notch signaling, was expressed in the a2-a3 joint epidermis.

1 Introduction

Hearing is important for animals, including insects, for perceiving their external environment and for mutual communication. For example, in *Drosophila*, males produce species-specific courtship songs through wing vibrations prior to mating, and females recognize conspecific songs, thereby facilitating copulation [1–3]. This form of acoustic communication is thought to play an important role in speciation [1, 4]. While most animals perceive sound through tympanic membranes, some insects, including flies and mosquitoes, detect sound via vibration of antennae located in antennae [5, 6]. The antenna consists of three large segments (a1 ~ 3), formed by the epidermis and the cuticle, an extracellular matrix composed of chitin and proteins that are deposited by the epidermis. The proximal region of a3 forms a thin tube that inserts into the invagination formed by a2. A feather-like structure (arista) is attached to a3 [2]. Since there are no muscles inserted into a2-a3 joint, its movement is mainly driven by external stimuli such as air vibrations [7]. Sounds cause vibration of the arista, which in turn causes rotation of a3. The rotation is sensed by the Johnston's organ (JO), which is housed in a2and is attached to the cuticle of the a2-a3 joint [2, 6, 8, 9]. JO consists of functional subunits called scolopidia [10]. Each scolopidium includes mechanosensory neurons, a ligament cell, a scolopale cell, a cap cell, and a dendritic cap [8]. The dendritic cap, an extracellular matrix secreted by the scolopale cell, covers the tips of the neurons and attaches to the cuticle [11–13].

The morphology of the a2-a3 joint and the attachment of JO to the joint are therefore crucial for the hearing function. In fact, mutations that disrupt these structures are associated with hearing deficits. For example, mutations in *atonal* (*ato*), a proneural gene encoding a basic helix-loop-helix transcription factor, cause severe aberrations of the a2-a3 joint morphology and abolish sound-induced a3 vibration

[14]. Loss of *spalt-major* (*salm*) and *spalt-related* (*salr*), which encoding zinc finger transcription factors, causes malformation of the joint and degeneration of scolopidia, resulting in hearing defects [10]. Likewise, a mutant for *cut* (*ct*), which encodes a homeodomain transcription factor, shows absence of the a2-a3 joint and is deaf [15]. These examples highlight the importance of joint morphogenesis in establishing the hearing function. While past studies have revealed the expression patterns of the relevant genes in the larval antennae and the ultimate morphological defects in mutant adults, morphogenetic processes during the intervening period, the pupal stage which lasts about 5 days, have remained largely unknown. Here we tracked antenna development in *Drosophila melanogaster* during the pupal stage, with focus on the a2-a3 joint and its association with JO. We describe the invagination of the epidermis that forms the joint structure, and subsequent deposition of the cuticle. Then we describe JO development in relation to the epidermal morphogenesis to show how JO establishes attachment to the a2-a3 joint. Lastly, we identified an enhancer trap that was expressed in the a2-a3 joint epidermis. These results will serve as a basis for understanding the molecular mechanism that forms the hearing structure.

2 Materials and methods

2.1 Fly strains

Fly strains used were: *Distal-less*^{md23} (*Dll*-GAL4) [16] (FBal0054121), *nompA.GFP*$^{5-3}$ (*GFP-NompA*) [12] (FBal0121650), *prospero*^{V1} (*pros*-GAL4) [17] (FBal0090504), *big brain* (*bib*)^{NP5149} (*bib*-GAL4) [18, 19] (FBal0224095), *fringe*^{NP6586} (*fng*-GAL4) [18, 19] (FBal0350314), *neuralized*^{NP1357} (*neur*-GAL4) [18] (FBti0034420), Canton-Special (Canton-S) (FBst0304357), UAS-*bib* RNAi^{JF02771}) (FBal0242353), UAS-mCD8::GFP.L^{LL5} (FBti0012685), UAS-mCD8::GFP.L^{2} (FBti0180511), UAS-mCD8.ChRFP^{2} (FBti0115768), 10XUAS-IVS-mCD8::RFP^{attP40} (FBti0131967), UAS-mCD8.mRFP.LG^{18a} (FBti0115748), and 20XUAS-IVS-mCD8::GFP^{attP2} (FBti0131936).

2.2 Tissue staining, confocal microscopy and image analysis

Pupal heads were dissected in phosphate buffer saline (PBS) and transferred to 4% paraformaldehyde in PBS. After removal of pupal cuticles, the antennae were fixed for 15–20 minutes at room temperature and washed with PBS. They were then mounted on glass slides, either directly or after staining as described below. For tissue staining, fixed antennae were stained in 0.3% Triton X-100 in PBS containing fluorescent dyes listed below at room temperature for 20–30 minutes. After staining, the samples were washed by PBS. Chitin was stained by Calcofluor White (Biotium). Actin was stained by Acti-stain 555 phalloidin or Acti-stain 647 phalloidin (Cytoskeleton Inc.). Confocal images of the antennae were captured on Olympus FV-3000. The acquired images were analyzed and processed on FV31S-SW image data viewing software. The lengths of dendritic caps, as labeled by GFP-NompA, were measured using the ImageJ plug-in Simple Neurite Tracer (SNT), which allows tracking of tube-like structures in 3D data

[20]. Three antennae were used for each time point. For each antenna, 10 dendritic caps which showed less than 10° tilt relative to the scanning plane were randomly selected for measurement.

3 Results

3.1 Morphogenesis of the antennal epidermis

We first tracked epidermal morphogenesis of the antenna during the pupal stage (Fig. 1). *Distal-less* (*Dll*)-GAL4 was used to drive the expression of a membrane-targeted EGFP throughout the epidermis of a2, a3 and the arista. The antennal primordium, which appeared as a flat disc at late third instar larva, gradually underwent deformation. At approximately 12 hours after puparium formation (APF), with the head inverted [21], the antennae were positioned dorsal to the eyes and had dome-like shapes (Fig. 1a, a'). Consistently with the previous report [21], at around 15 hours APF, they began to move towards the anterior tips of the head. The movement was accompanied by elongation of the arista (Fig. 1b-d), whose tip continued to be anchored to the pupal cuticle [22]. The antennal movement ceased and the arista reached its maximum length at about 22 hours APF. The a2-a3 joint appeared as a simple epithelial constriction during these stages (arrowheads in Fig. 1a'-d'). Subsequently, the joint gradually decreased in diameter and invaginated dorsally into the a2 segment. The invagination proceeded asymmetrically, with the lateral region invaginating deeper than the medial region. The asymmetry was already present at 23–25 hours APF (Fig. 1e, e') and grew larger (Fig. 1f-h') so that at 36–38 hours APF, the joint was oriented parallel to the dorsoventral axis (Fig. 1i, i'). The diameter of the joint continued to decrease (Fig. 1j-m). At 54 hours APF, its inner diameter was approximately 10μm. In three dimensions, the joint formed a ring-like structure (Fig. 1n).

In the leg, deposition of the adult cuticle began at 45–48 hours APF [19]. In the antenna, cuticle formation had not begun at 45 hours APF, as revealed by the absence of chitin, a major component of the cuticle (Fig. 2a). At 47 hours APF, patchy chitin signals were found on bristles on the external surface of a2 and a3, but not in the a2-a3 joint (Fig. 2b). At 54 hours, cuticle had formed throughout the apical surface of the a2-a3 joint epidermis (Fig. 2c).

3.2 The development of Johnston's organ (JO) in relation to the epidermal morphogenesis

We next observed the formation and morphogenesis of JO, with a focus on its connection to the epidermis and/or the cuticle. The JO consists of functional subunits called scolopidia [10]. Each scolopidium is composed of chordotonal neurons, a ligament cell, a scolopale cell, a cap cell, and a dendritic cap (Fig. 3a) [8]. The dendritic cap, an extracellular matrix that covers the tips of the neurons and connects them to the a2-a3 joint cuticle in the mature JO, was visualized by GFP-NompA (Fig. 3a') [11–13]. The scolopale cell, which envelops the dendrites of the neurons and which secretes the dendritic cap, contains actin-rich structures known as scolopale rods [6, 23, 24]. The cap cell also contains actin-rich structures called cap rods [6]. The scolopale rods and the cap rods can be visualized

by actin staining, simultaneously with the actin-rich apical cortex of the epidermis (Fig. 3a') [6]. *prospero* (*pros*) encodes an evolutionary conserved atypical homeodomain protein that is expressed in the scolopale cells [12, 25, 26]. We used *pros*-GAL4 to drive the expression of a membrane-targeted fluorescent protein to visualize the scolopale cell membrane (Fig. 3a').

At 10 hours APF, *pros*-GAL4 was expressed in scolopale cells, while GFP-NompA was not detected (Fig. S1a). We found a thin protrusion on each scolopale cell, and a rod-like actin structure in the protrusion (Fig. 3b). The actin structures were likely to be scolopale rods, because they were enclosed by the scolopale cell membrane (Fig. 3b'). At 14 hours APF, GFP-NompA was detected in a subset of scolopale cells (Fig. S1b). GFP-NompA was localized not only in the cell body but also at the tip of the cell protrusion, extending out of the cell membrane (Fig. 3c, c'), indicating that a fraction of GFP-NompA had been deposited extracellularly. Actin signals were found both inside and outside of the scolopale cell protrusions (Fig. 3c'). The portion of the actin structure that resides outside of the scolopale cells were presumed to be cap rods. The cap rods extended beyond the GFP-NompA structures (Fig. 3c', c"). At 21 hours APF, GFP-NompA was detected in all scolopidia lining the epidermal invagination of the a2-a3 joint (Fig. S1c, c'). The tip of the GFP-NompA structure was found at the level of the apical actin network of the epidermis, indicating that the dendritic cap had elongated to reach the cap rod tip located at the level of the epidermal apical surface (Fig. 3d, d'). The dendritic cap tip continued to be positioned at the apical surface of the epidermis afterwards (Fig. 3e, f). Simultaneous labeling of the scolopale cell membrane revealed that the dendritic cap extended further beyond the tip of the scolopale cell protrusion than at 14 hours APF (compare Fig. 3e, f with Fig. 3c'). The rapid elongation of the dendritic cap was corroborated by analyzing the lengths of GFP-NompA structures over time, which showed a rapid increase between 38 and 44 hours APF (Fig. 4). At 46 hours APF, some dendritic caps showed bending near the apical tips (Fig. 3g). This could be due to the changes in the overall epidermal morphology (Fig. 3g'), resulting from deepening of the epidermal invagination at this stage, as described above (Fig. 1k-l).

In the course of these observations, we noticed that some scolopidia detached from the cuticle in flies that harbor the *GFP-NompA* transgene, even in the otherwise normal background. At 27 hours APF, while most scolopidia were aligned along the a2-a3 joint and contacted the apical surface of the epidermis as described above, a subset of scolopidia were displaced from the normal alignment and were not in contact with the epidermis (Fig. 5a-b), The detachment appeared to be more prominent at 44 hours APF (Fig. 5c, d). The detachment could result from aberrant function of GFP-NompA: it was previously reported that addition of GFP to the N-terminal of NompA interfered with adhesion of the dendritic cap to the cuticle [12].

3.3 Expression of Notch target genes in the antenna

We previously showed that *big brain* (*bib*)-GAL4, *fringe* (*fng*)-GAL4, and *neuralized* (*neur*)-GAL4, which are enhancer traps of target genes of Notch signaling, were expressed in distinct cell populations within joints in the leg, an organ serially homologous to the antenna [19, 27]. Here we examined their

expression in the antenna by expressing a membrane-targeted fluorescent protein under the control of these GAL4 drivers.

We found that *bib*-GAL4 was expressed in the epidermis around the a2-a3 joint. In the dome-shaped antenna at 12–13 hour and 15–17 hours APF, *bib*-GAL4 expression was observed in a circular band of cells immediately distal to the a2-a3 joint, marked by the developing scolopidia (Fig. 6a-b'). *bib*-GAL4 expression did not overlap JO but abutted the distal side of JO (Fig. 6a-b'). From 17–19 hours APF onward, *bib*-GAL4 was expressed in both distal and proximal sides of the epidermal invagination of the a2-a3 joint (Fig. 6c-f), suggesting that *bib*-GAL4 expression expanded proximally. A spatial shift in *bib*-GAL4 expression during pupal development has also been described in the leg joint [28]. *bib*-GAL4 expression continued to be restricted to the epidermis and excluded from the JO (Fig. 6d'). *bib*-GAL4 was also expressed in a separate, proximal region corresponding to the a1-a2 joint (Fig. 6a-f). To assess the function of *bib*, we conducted *bib* knockdown by expressing a double-stranded RNA against *bib* with *bib*-GAL4. No apparent morphological abnormalities were observed in either the a2-a3 joint or the JO (Fig. S2).

fng-GAL4 was expressed in the a2 epidermis excluding the a1-a2 and a2-a3 joint regions where *bib*-GAL4 was expressed (Fig. 7a). *neur*-GAL4 was expressed in JO neurons but not in the epidermis (Fig. 7b), in contrast to the leg joint, where *neur*-GAL4 was expressed in the epidermis [19].

Figure 7. Expression of *fng*-GAL4 and *neur*-GAL4. **(a)** A representative antenna at 36–38 hours APF, in which the expression of a membrane-targeted GFP is driven by *fng*-GAL4 is stained for actin and viewed along the anterior-posterior axis. **(a')** A schematic drawing of *fng*-GAL4 expression in relation to *bib*-GAL4 expression. Whether the two drivers are expressed in an exactly complementary manner is not clear. **(b, b')** A representative antenna at 36–38 hours APF in which *neur*-GAL4 is used to express the membrane-targeted GFP, stained and viewed as in (a). A magnified view of the boxed region in (b) is shown in (b'). GFP is expressed in JO neurons, extending into the actin-rich scolopale and cap rods that are connected to the a2-a3 joint (arrowhead). GFP

expression is not detected in the epidermis (epi, double-headed arrows). Asterisk indicates axons extending from a3. (a) is flipped horizontally. Scale bars: 50 μm in (a, b), 10 μm in (b').

4 Discussion

4.1 The relationship between JO and the a2-a3 joint

Previous reports implied mutual developmental influence between the JO and the a2-a3 joint. The proneural gene *ato* is expressed in the larval antennal primordium specifically in sensory organ precursor cells (SOPs) fated to become chordotonal organs including JO, and is required for their development [29, 30]. Loss of *ato* function results not only in the deprivation of JO, but alterations in the cuticle morphology of the a2-a3 joint, which abolish a3 mobility [14, 30]. These observations are consistent with the contribution of JO in regulating the development of the a2-a3 joint epidermis and cuticle, although

we cannot exclude the possibility that *ato* directly regulates joint development. The transcription factor gene *ct* is expressed in presumptive a2 epidermis. Loss of *ct* function directly causes cuticular defects in the a2-a3 joint and loss of a3 mobility, but it does not interfere with the differentiation of scolopidia. Instead, scolopidia that have once formed in *ct* mutants undergo subsequent degeneration [15]. Similarly, flies doubly mutant for *salm* and *salr* show defects in the a2-a3 joint cuticle morphology, initially normal differentiation of scolopidia, and their subsequent degeneration [10]. These observations suggest that normal development of the a2-a3 joint cuticle is crucial for the maintenance of JO.

Our present findings shed light on how JO may influence the epidermal/cuticular structure of the a2-a3 joint. The tips of dendritic caps marked by GFP-NompA gradually elongated and reached the tips of the cap rods at 21 hours APF, forming integral tips of scolopidia at the epidermal apical cortex of the a2-a3 joint (Fig. 3d). From this stage onward, the tips of scolopidia continued to be located precisely at the deepest point of the epidermal invagination of the joint (Fig. 4d'). This raises the possibility that JO induces epidermal invagination by mechanically pulling the epidermis or by sending a biochemical signal. Consistently, *ato* mutants showed incomplete epidermal invagination at the a2-a3 joint [14]. Studying the course of epidermal morphogenesis in *ato* mutants, in comparison to the wild-type development that we described here, will provide insight into the mechanical or biochemical mechanisms by which JO regulates the joint morphology.

How the a2-a3 joint contributes to the maintenance of JO is more enigmatic. In a *ct* mosaic antenna, scolopidia that consisted of wild-type cells and neighbored a *ct* mutant clone were displaced away from the epidermis at approximately 40 hours APF [15], which was prior to the onset of cuticle formation (our present study, Fig. 2). These results firstly indicate that scolopidia need anchorage in order to stay at the normal position along the epidermis. Secondly, the anchorage occurs before cuticle is formed. Lastly, the anchorage requires the function of *ct* outside of the scolopidia. While the transmembrane protein NompA is reported to mediate attachment to the cuticle [12], what anchors scolopidia to the epidermis in the absence of cuticle is elusive. Temporal analysis of *ct* mutants to study morphological changes of the scolopidia and the epidermis as well as changes in their spatial relationship prior to cuticle formation, and comparing them to the changes in the wild-type animal described in this study, will provide the basis for addressing the question.

4.2 Dendritic cap rapid elongation

We analyzed the formation of the dendritic cap, the extracellular matrix that ultimately connects the tips of the neuronal cilia to the cuticle, by labeling its component NompA with GFP. We showed that GFP-NompA elongated rapidly between about 38 and 44 hours APF (Fig. 4). What drives the rapid elongation? From 14 hours to 32 hours APF, GFP-NompA was detected in the scolopale cell bodies (Fig. 3c-e). At 44 hours APF, GFP-NompA signals were substantially reduced in the cell bodies (Fig. 3f). Therefore, NompA transport from the cell bodies to the protrusions of scolopale cells, followed by its secretion from the protrusions, may partially account for the rapid elongation. In addition, tension imposed on the dendritic caps may contribute to their rapid elongation. As discussed above, JO may drive epidermal invagination by mechanically pulling the epidermis. The tension created by the pulling may drive dendritic cap

elongation. The source of the pulling force is presently unclear. The basal side of scolopidia (the side opposite to the dendritic caps) is attached to the cuticle of the proximal region of a2 via the ligament cells [23]. The pulling on the scolopidia may therefore result from morphological changes in the a2 epidermis/cuticle, which bridge the two ends of a scolopidium. How and when the ligament cells become connected to proximal a2, and how a2 morphology changes afterwards, need to be addressed in the future.

4.3 JO detachment in *GFP-NompA* flies

We observed detachment of scolopidia from the a2-a3 joint in flies harboring *GFP-NompA*. The detachment was found at 27 hours APF and appeared more prominent at 47 hours APF (Fig. 5). As mentioned above, the addition of GFP to NompA is reported to interfere with adhesion between the dendritic cap and the cuticle [12]. Detachment of the scolopidia in *GFP-NompA* flies at 27 hours APF, which is before cuticle is formed, again supports the possibility raised above that scolopidia are anchored to the a2-a3 joint epidermis prior to the onset of cuticle formation.

Declarations

Author information

Authors and affiliations

Graduate School of Science and Engineering, Chiba University, Chiba, 263–8522 Japan.

Shan Jiang

Graduate School of Science, Chiba University, Chiba, 263–8522 Japan.

Reiko Tajiri

Contributions

S.J. and R.T. conceived the project. S.J. conducted experiments and data analysis and prepared the first draft of the manuscript. R.T. revised the manuscript. Both authors read and approved the manuscript.

Corresponding author

Correspondence to Reiko Tajiri (rtajiri@chiba-u.jp)

Ethics declarations

Ethics approval

Not applicable.

Consent to participate

Not applicable.

Consent for publication

Not applicable.

Competing interests

The authors declare no competing interests.

Clinical trial number

Not applicable

Funding

This work was supported by JST SPRING, Grant Number 190PT01056, through the All Directional Innovative Challenger Ph.D. (ALDIC-PhD) project, Chiba University, to S.J. and by Suntory SunRiSE program (Suntory Rising Stars Encouragement Program in Life Sciences) to R.T.

Author Contribution

S.J. and R.T. conceived the project. S.J. conducted experiments and data analysis and prepared the first draft of the manuscript. R.T. revised the manuscript. Both authors read and approved the manuscript.

Acknowledgement

We thank Masumi Nitanda and Kyoko Chagi for technical support, Tajiri lab colleagues for helpful discussion, and the Kyoto Stock Center and the Bloomington Stock Center for providing fly strains.

Data Availability

All data supporting the findings of this study are available within the paper and its Supplementary Information.

References

1. Greenspan RJ, Ferveur JF (2000) Courtship in *Drosophila*. Annu Rev Genet 34:205–232. https://doi.org/10.1146/annurev.genet.34.1.205
2. Ishikawa Y, Kamikouchi A (2016) Auditory system of fruit flies. Hear Res 338:1–8. https://doi.org/10.1016/j.heares.2015.10.017
3. Ohashi TS, Ishikawa Y, Awasaki T, Su MP, Yoneyama Y, Morimoto N et al (2023) Evolutionary conservation and diversification of auditory neural circuits that process courtship songs in *Drosophila*. Sci Rep 13(1):383. https://doi.org/10.1038/s41598-022-27349-7
4. Chen A, Chen C, Katoh T, Katoh TK, Watada M, Toda MJ et al (2019) Evolution and diversity of the courtship repertoire in the *Drosophila* montium species group (Diptera: Drosophilidae). J Evol Biol 32(10):1124–1140. https://doi.org/10.1111/jeb.13515
5. Boo KS, Richards AG (1975) Fine structure of the scolopidia in the Johnston's organ of male *Aedes aegypti* (L.) (Diptera: Culicidae). Int J Insect Morphol Embryol 4(6):549–566. https://doi.org/10.1016/0020-7322(75)90031-8
6. Boekhoff-Falk G, Eberl DF (2014) The *Drosophila* auditory system. WIREs Dev Biol 3(2):179–191. https://doi.org/10.1002/wdev.128
7. Suver MP, Medina AM, Nagel KI (2023) Active antennal movements in *Drosophila* can tune wind encoding. Curr Biol 33(4):780–789e4. https://doi.org/10.1016/j.cub.2023.01.020
8. Eberl DF, Boekhoff-Falk G (2007) Development of Johnston's organ in *Drosophila*. Int J Dev Biol 51(6–7):679–687. https://doi.org/10.1387/ijdb.072364de
9. Albert JT, Nadrowski B, Göpfert MC (2007) Mechanical signatures of transducer gating in the *Drosophila* ear. Curr Biol 17(11):1000–1006. https://doi.org/10.1016/j.cub.2007.05.004
10. Dong PDS, Todi SV, Eberl DF, Boekhoff-Falk G (2003) *Drosophila spalt/spalt-related* mutants exhibit Townes-Brocks' syndrome phenotypes. Proc Natl Acad Sci 100(18):10293–10298. https://doi.org/10.1073/pnas.1836391100
11. Fernandes I, Chanut-Delalande H, Ferrer P, Latapie Y, Waltzer L, Affolter M et al (2010) Zona pellucida domain proteins remodel the apical compartment for localized cell shape changes. Dev Cell 18(1):64–76. https://doi.org/10.1016/j.devcel.2009.11.009
12. Chung YD, Zhu J, Han YG, Kernan MJ (2001) *nompA* encodes a PNS-specific, ZP domain protein required to connect mechanosensory dendrites to sensory structures. Neuron 29(2):415–428. https://doi.org/10.1016/S0896-6273(01)00215-X
13. Uga S, Kuwabara M (1965) On the fine structure of the chordotonal sensillum in antenna of *Drosophila melanogaster*. J Electron Microsc (Tokyo) 14(3):173–181. https://doi.org/10.1093/oxfordjournals.jmicro.a049481
14. Göpfert MC, Stocker H, Robert D (2002) *atonal* is required for exoskeletal joint formation in the *Drosophila* auditory system. Dev Dyn. ;225(1):106–109. https://doi.org/10.1002/dvdy.10136
15. Ebacher DJS, Todi SV, Eberl DF, Boekhoff-Falk GE (2007) *cut* mutant *Drosophila* auditory organs differentiate abnormally and degenerate. Fly (Austin). ;1(2):86–94. https://doi.org/10.4161/fly.4242

16. Calleja M, Moreno E, Pelaz S, Morata G (1996) Visualization of gene expression in living adult *Drosophila*. Science 274(5285):252–255. https://doi.org/10.1126/science.274.5285.252
17. Balakireva M, Stocker RF, Gendre N, Ferveur JF (1998) Voila, a new *Drosophila* courtship variant that affects the nervous system: behavioral, neural, and genetic characterization. J Neurosci 18(11):4335–4343. https://doi.org/10.1523/JNEUROSCI.18-11-04335.1998
18. Hayashi S, Ito K, Sado Y, Taniguchi M, Akimoto A, Takeuchi H et al (2002) GETDB, a database compiling expression patterns and molecular locations of a collection of Gal4 enhancer traps. Genesis 34(1–2):58–61. https://doi.org/10.1002/gene.10137
19. Tajiri R, Misaki K, Yonemura S, Hayashi S (2010) Dynamic shape changes of ECM-producing cells drive morphogenesis of ball-and-socket joints in the fly leg. Development 137(12):2055–2063. https://doi.org/10.1242/dev.047175
20. Longair MH, Baker DA, Armstrong JD (2011) Simple Neurite Tracer: open source software for reconstruction, visualization and analysis of neuronal processes. Bioinformatics 27(17):2453–2454. https://doi.org/10.1093/bioinformatics/btr390
21. Lienhard MC, Stocker RF (1991) The development of the sensory neuron pattern in the antennal disc of wild-type and mutant (*lz*^{3}, *ssa*) *Drosophila melanogaster*. Development 112(4):1063–1075. https://doi.org/10.1242/dev.112.4.1063
22. Ray RP, Matamoro-Vidal A, Ribeiro PS, Tapon N, Houle D, Salazar-Ciudad I et al (2015) Patterned anchorage to the apical extracellular matrix defines tissue shape in the developing appendages of *Drosophila*. Dev Cell 34(3):310–322. https://doi.org/10.1016/j.devcel.2015.06.019
23. Todi SV, Sharma Y, Eberl DF (2004) Anatomical and molecular design of the *Drosophila* antenna as a flagellar auditory organ. Microsc Res Tech 63(6):388–399. https://doi.org/10.1002/jemt.20053
24. Wolfrum U (1997) Cytoskeletal elements in insect sensilla. Int J Insect Morphol Embryol 26(3):191–203. https://doi.org/10.1016/S0020-7322(97)00021-4
25. Reddy GV, Rodrigues V (1999) Sibling cell fate in the *Drosophila* adult external sense organ lineage is specified by Prospero function, which is regulated by. Numb Notch Dev 126(10):2083–2092. https://doi.org/10.1242/dev.126.10.2083
26. Manning L, Doe CQ (1999) Prospero distinguishes sibling cell fate without asymmetric localization in the *Drosophila* adult external sense organ lineage. Development 126(10):2063–2071. https://doi.org/10.1242/dev.126.10.2063
27. Tajiri R, Misaki K, Yonemura S, Hayashi S (2011) Joint morphology in the insect leg: evolutionary history inferred from notch loss-of-function phenotypes in *Drosophila*. Development 138(21):4621–4626. https://doi.org/10.1242/dev.067330
28. Shirai T, Yorimitsu T, Kiritooshi N, Matsuzaki F, Nakagoshi H (2007) Notch signaling relieves the joint-suppressive activity of defective proventriculus in the *Drosophila* leg. Dev Biol 312(1):147–156. https://doi.org/10.1016/j.ydbio.2007.09.003
29. Jarman AP, Grau Y, Jan LY, Jan YN (1993) *atonal* is a proneural gene that directs chordotonal organ formation in the *Drosophila* peripheral nervous system. Cell. ;73(7):1307–1321.

https://doi.org/10.1016/0092-8674(93)90358-W

30. Jarman AP, Sun Y, Jan LY, Jan YN (1995) Role of the proneural gene, *atonal*, in formation of *Drosophila* chordotonal organs and photoreceptors. Development 121(7):2019–2030. https://doi.org/10.1242/dev.121.7.2019

Figures

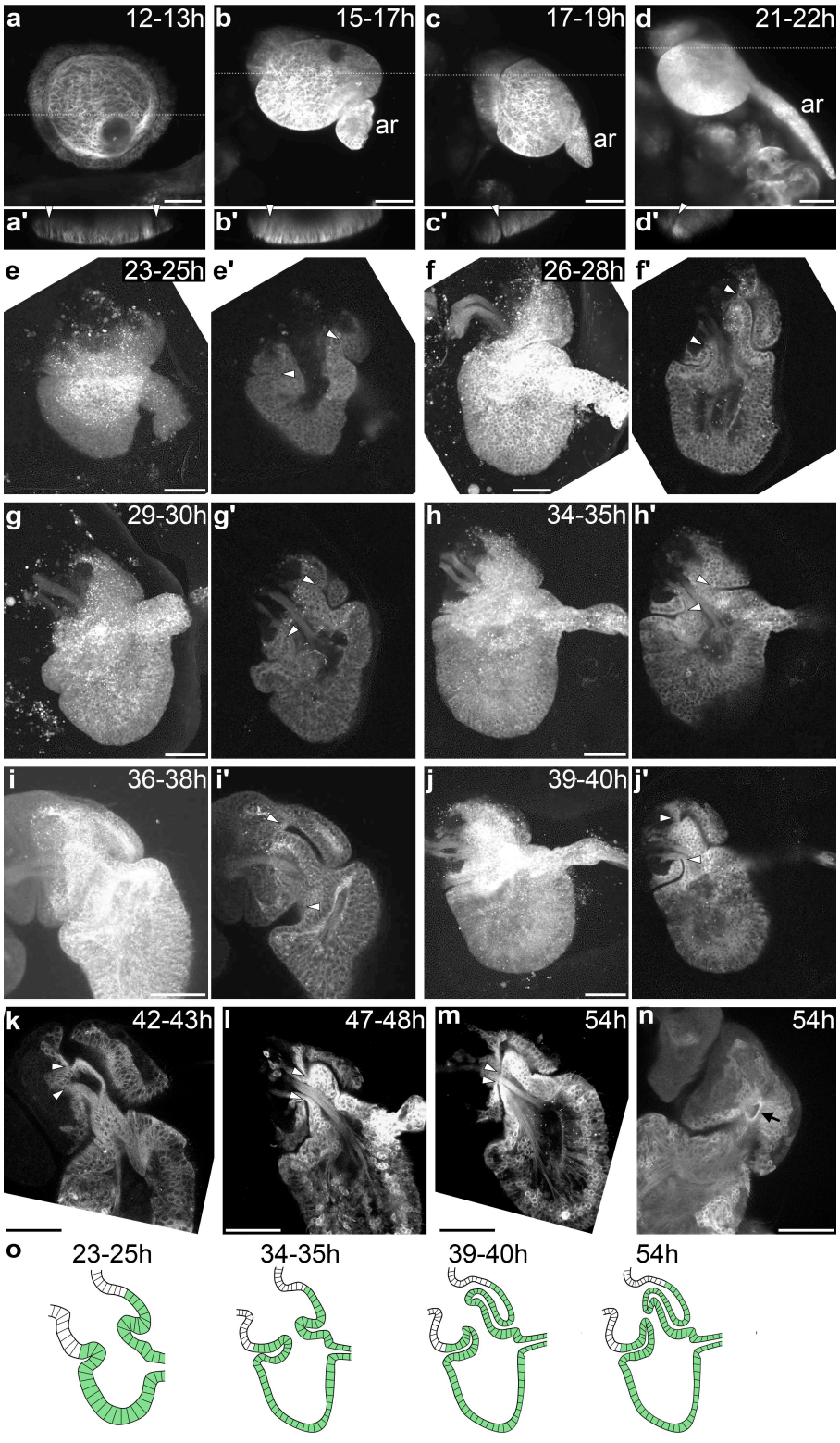


Figure 1

Morphogenesis of the antennal epidermis during the pupal stage. The epidermal cell membranes of a2, a3 and the arista are labeled by *Dll*-GAL4-driven expression ofmCD8::GFP (a-h, j-n) or mCD8::mChRFP(i). **(a-d)** Antennae observed from their distal sides in live pupae at indicated hours APF. ar, aristae. **(a'-d')** Optical cross-sections along the dotted lines in (a-d), oriented with the apical sides of the epidermis downward. Arrowheads indicate epithelial constrictions of the a2-a3 joint. **(e-m)** Fixed antennae from pupae at indicated hours APF, observed along the anterior-posterior axis. Distal is downward and lateral is to the right. Z stacks (e-j) or single focal planes roughly at the centers of the antennae (e'-j', k-m) are shown. Arrowheads indicate epidermal invagination of the a2-a3 joint. **(n)** An antenna fixed at 54 hours APF, observed along the lateral-medial axis. The slice parallel to the a2-a3 joint shows the circular shape of the invagination (arrow). (o) Schematic diagram of epidermal morphogenesis. Cells expressing *Dll*-GFP are shown in green. In (d-g') and (k, l), imageswere horizontally flipped so that the lateral sides are oriented to the right in all panels. Scale bars: 50 μm.

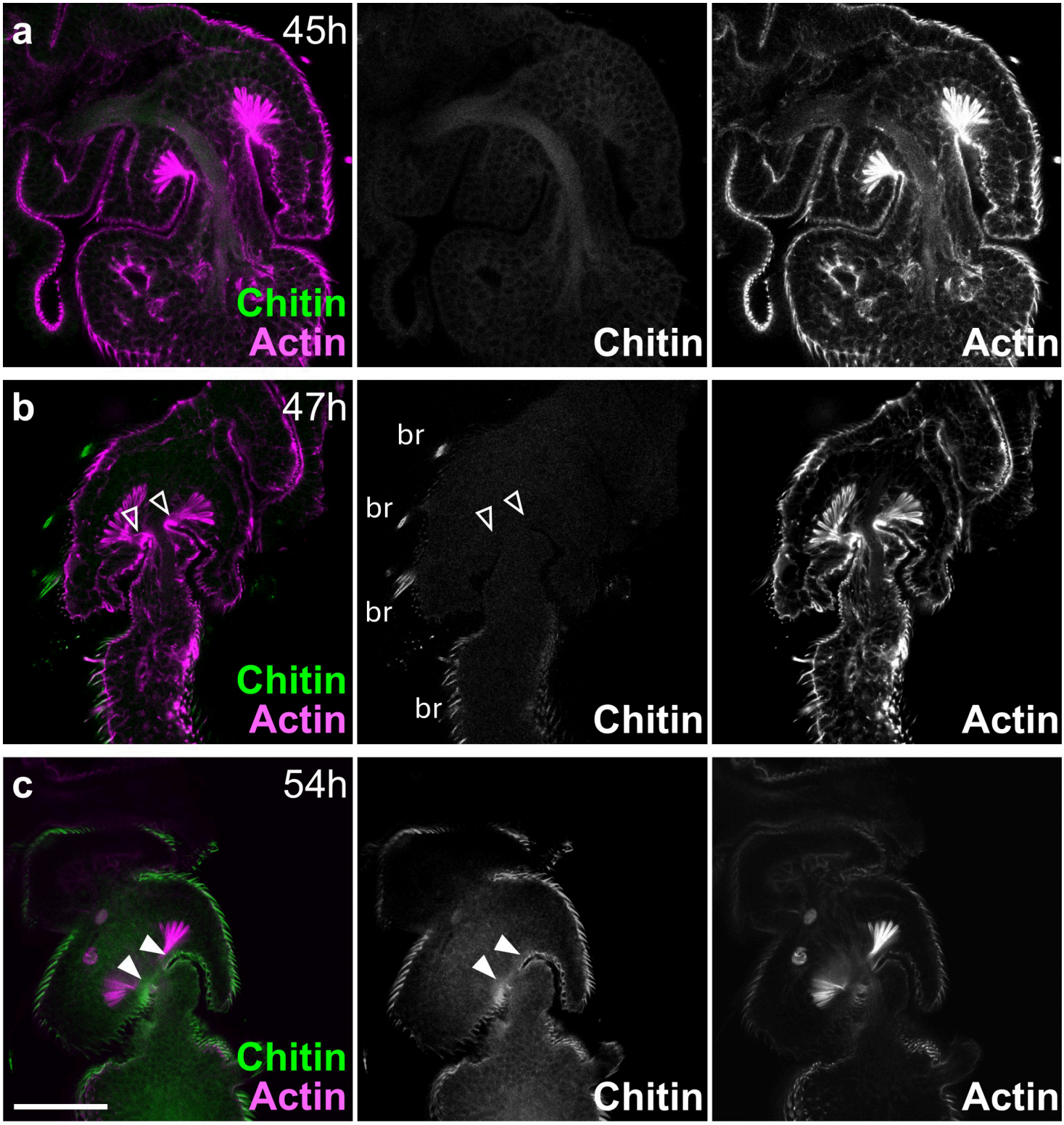


Figure 2

Cuticle formation. **(a-c)** Single focal planes of antennae fixed at indicated hours APF and stained for chitin and actin. At 45 hours APF,chitin is not detected above the background level throughout the antenna (a). At 47 hours APF, chitin signals areobserved on some bristles (br), but not at the a2-a3 joint (open arrowheads), marked by actin structures (cap rods and scolopale rods) of JO (b). At 54 hours

APF,chitin signals are detected at the a2-a3 joint (closed arrowheads in (c)). In (c), images were horizontally flipped so that the lateral sides are oriented to the right. Scale bar: 50 μm.

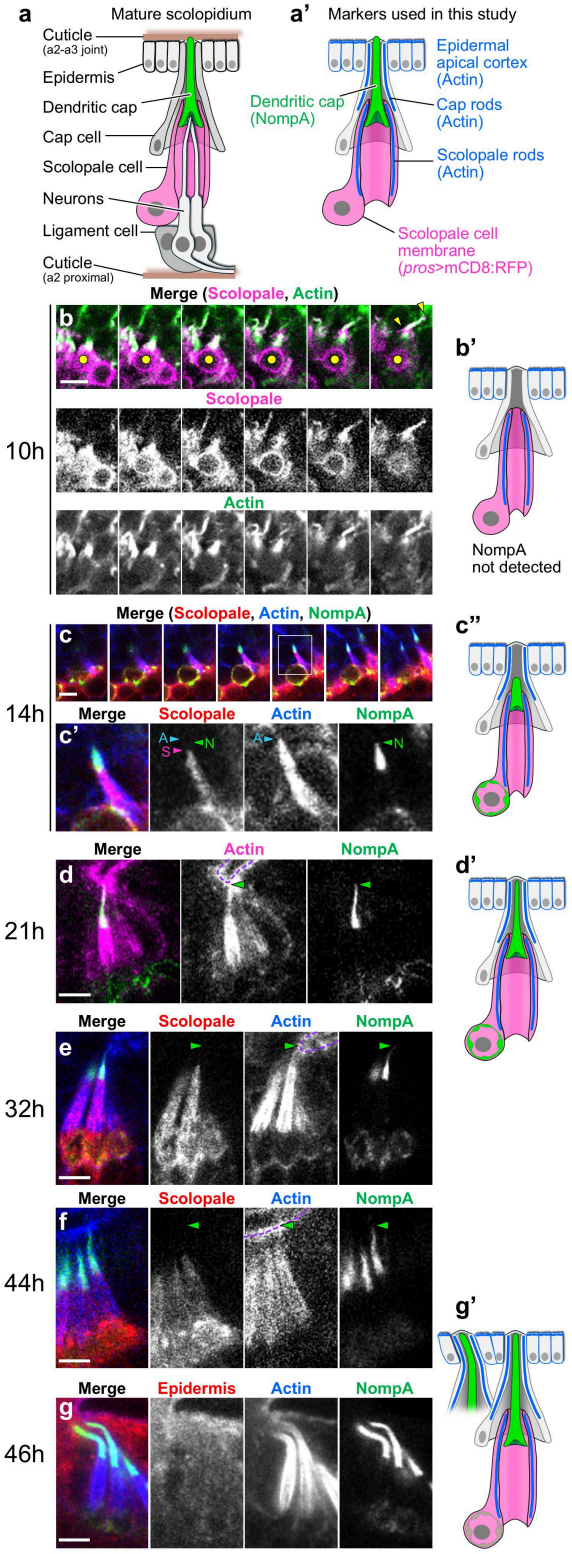


Figure 3

Morphogenesis of JO. **(a, a')** Schematic drawings of a section of a mature scolopidium, modified from [6]. In this study, the scolopale cell membranes were visualized by *pros*-GAL4-driven expression of

mCD8::RFP, and dendritic caps were visualized by GFP-NompA. Actin constituting the scolopale rods, the cap rods and the apical cortex of the epidermiswas stained by phalloidin. See text for detail. **(b)** A series of confocal sections through a scolopidium at 10 hours APF. Scolopale cell membranes and actin are shown in magenta and green, respectively, in the merged images, and are shown separately in lower panels. Actin is detected within the scolopale cell protrusion (yellow arrowheads), extending from the scolopale cell body (yellow dots). **(b')** The scolopidium organization at 10 hours APF, deduced from (b). The scolopale rods, but not the cap rods, have formed. GFP-NompA is not detected (see Fig. S1). **(c)** Serial confocal sections at 14 hours APF, showing scolopale cell membranes in red, actin in blue and GFP-NompA in green. **(c')** Magnified view of the boxed region in (b). Arrowheads indicate the tip positionsof the scolopale cell protrusion (S, magenta), the actin structure (A, blue), and the dendritic cap labeled by GFP-NompA (N, green). **(c'')** The scolopidium structure at 14 hours APF, deduced from (c, c'). The cap rods have formed. NompA is secreted but has not reached the cap rod tips. **(d)** A confocal section through a scolopidium at 21 hours APF. Actin and GFP-NompA are shown in magenta and green, respectively, in the merged image, and in grayscale in separate images. Green arrowheads indicate the tip position of the dendritic cap, which is at the level of the epidermal apical cortex (purple dashed line). Note that the epidermis of this region has formed a sharp invagination. In (d-f), representative scolopidia whose entire extent is captured within a single confocal section are shown. **(d')** The scolopidium structure at 21 hours APF, deduced from (d). **(e, f)** Single confocal sections at 32 hours APF (e)and 44 hours APF (f). The position of the dendritic cap tip (green arrowheads) is at the level of the epidermal apical cortex (purple dashed lines). **(g)** A projection of three consecutive optical sections from a Z-stack acquired at 0.56-μm intervals of an antenna at 46 hours APF. The epidermis is labeled by *Dll*-GAL4-driven expression of mChRFP. **(g')**A drawing of scolopidia at 46 hours APF. Bending of some scolopidia could be attributed to changes in the epidermal morphology. Scale bars: 5μm.

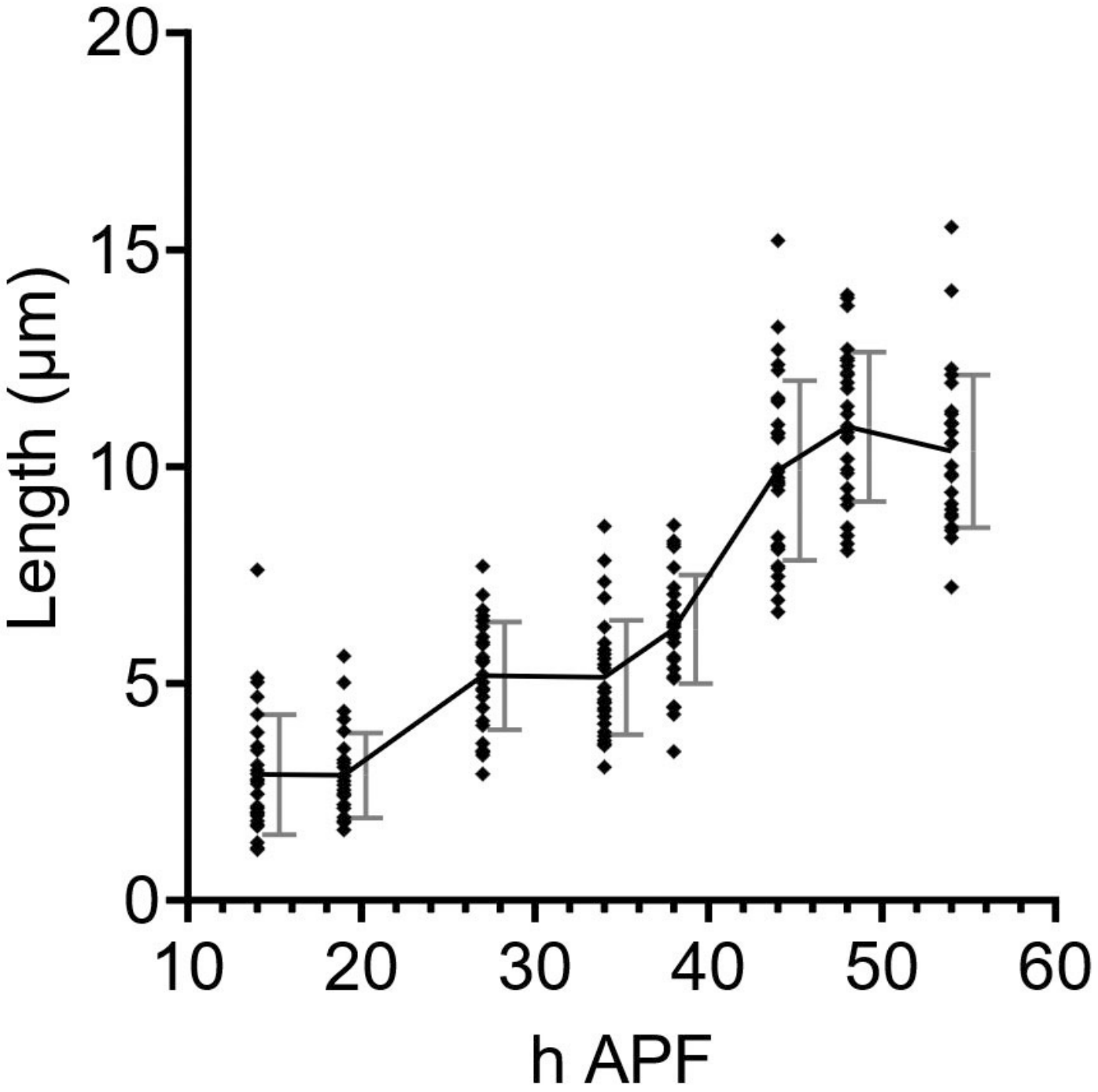


Figure 4

Dendritic cap length dynamics during the pupal stage. Dots represent the lengths of individual dendritic caps (10 dendritic caps per antenna, 3 antennae per time point). The black line connects the mean values at each time point, and error bars indicate S.D. See Materials and methods for detail.

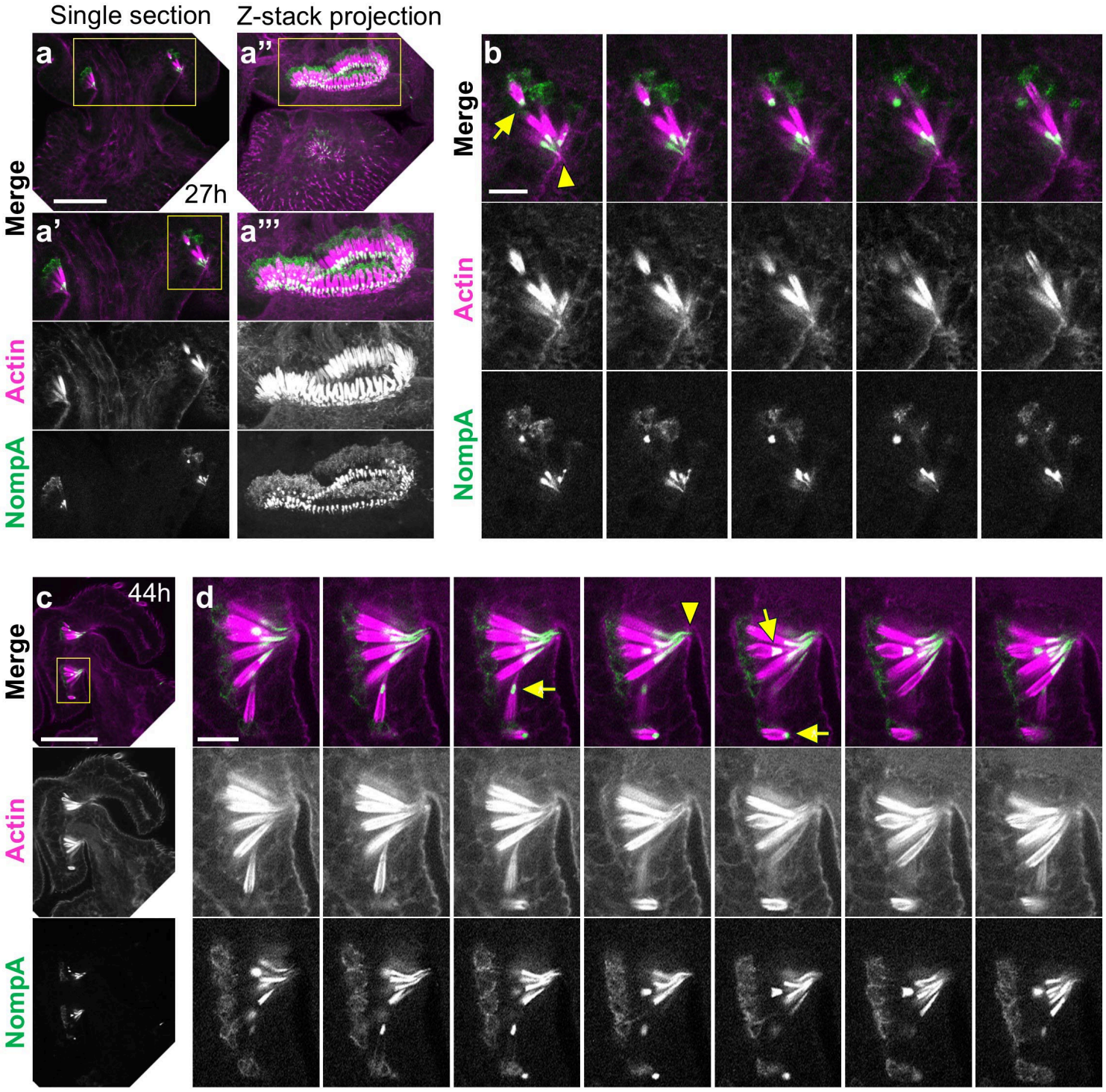


Figure 5

Scolopidia detachment in flies harboring *GFP-NompA*. Antennae of flies harboring one copy of the *GFP-NompA* transgene are stained for actin. **(a-a''')** An antenna at 27 hours APF. A single confocal section (a) and a Z-stack projection (a''), viewed along the anterior-posterior axis, are shown. (a') and (a''') are magnified views of the boxed region in (a) and (a''), respectively. **(b)**A series of confocal sections of the boxed region in (a'). **(c)** An antenna at 44hours APF. **(d)** A series of confocal sections of the boxed region in (c). In (b, d), arrowheads indicate the apical surface of the epidermis to which most scolopidia are

connected. Arrows indicate scolopidia that are unconnected to the epidermis and are displaced from the alignment of other scolopidia. All images are flipped horizontally. Scale bars: 50 μm in (a, c), 10 μm in (b, d).

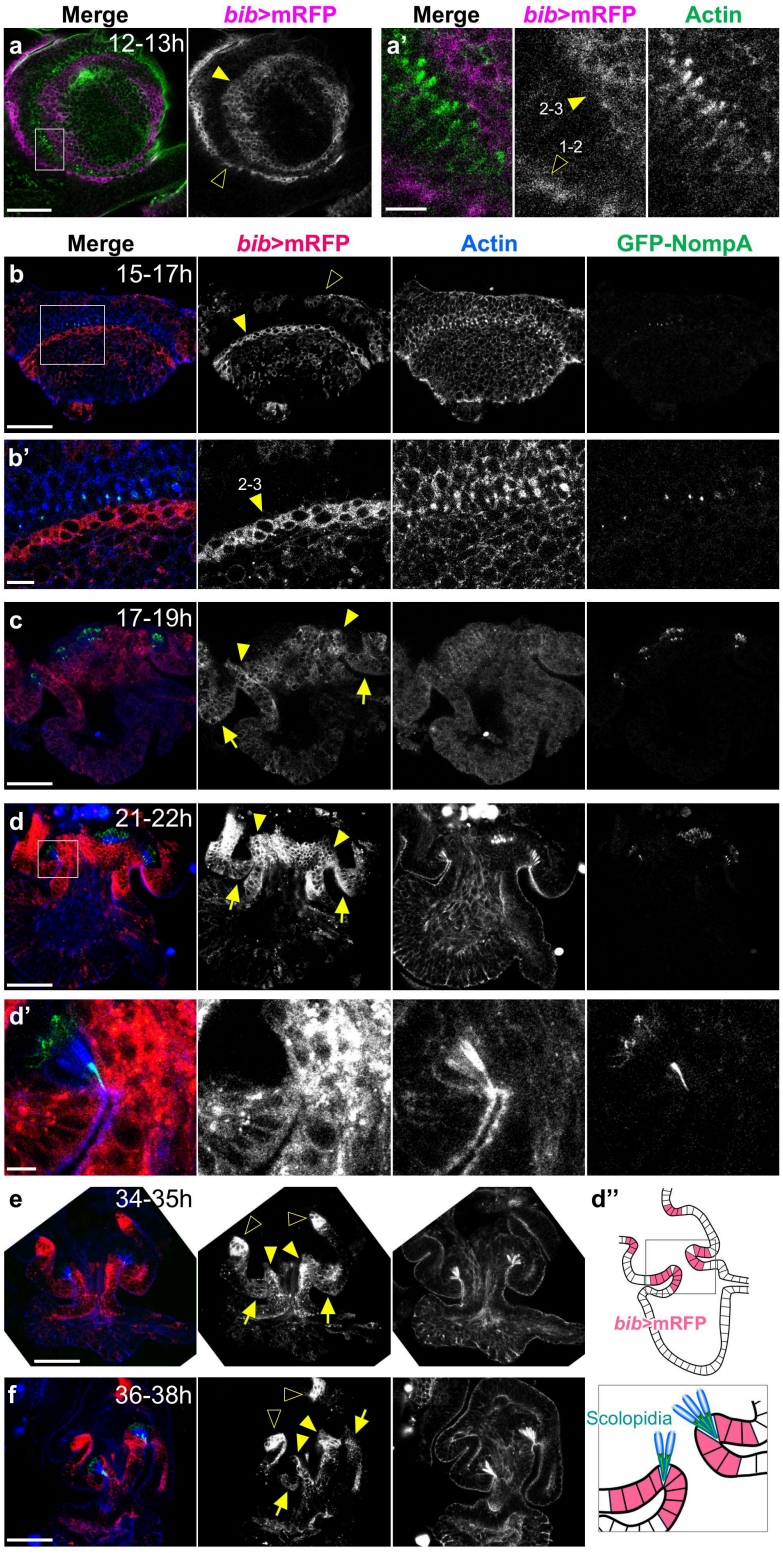


Figure 6

Expression of *bib*-GAL4 in the pupal antenna. *bib*-GAL4 is used to drive the expression of mCD8::mRFP. Scolopidia are visualized by GFP-NompA and actin staining. **(a-b')** The distal view of a representative dome-shaped antenna at 12-13 hours APF and viewed from its distal side (a, a'), or a side view of a dome-shaped antenna at 14-15 hours APF (b, b'). (a', b') show magnified views of the boxed regions in (a, b). Scolopidia, visualized by their actin rods (a-b') and dendritic caps (GFP-NompA in b, b'), mark the position of the a2-a3 joint. *bib*-GAL4 is expressed in a band of cells immediately distal to the a2-a3 joint (filled arrowheads), and in a more proximal circular band corresponding to the a1-a2 joint (open arrowheads). **(b-f)** Single confocal sections of antennae, representative of the indicated periods (hours APF). A magnified view of the boxed region in (d) is shown in (d'). *bib*-GAL4 is expressed not only on the distal side of the a2-a3 joint (filled arrowheads) but also on its proximal side (arrows). It continues to be expressed along the a1-a2 joint (open arrowheads). **(d'')** A drawing of *bib*-GAL4 expression in relation to the JO (scolopidia) at 21-22 hours APF. (d, d') shows the same antenna as in Fig. 3d and S1c, c'. Images in (d, d') are flipped horizontally. Scale bars: 10 μm in (a', b', d'), 50 μm in the other panels.

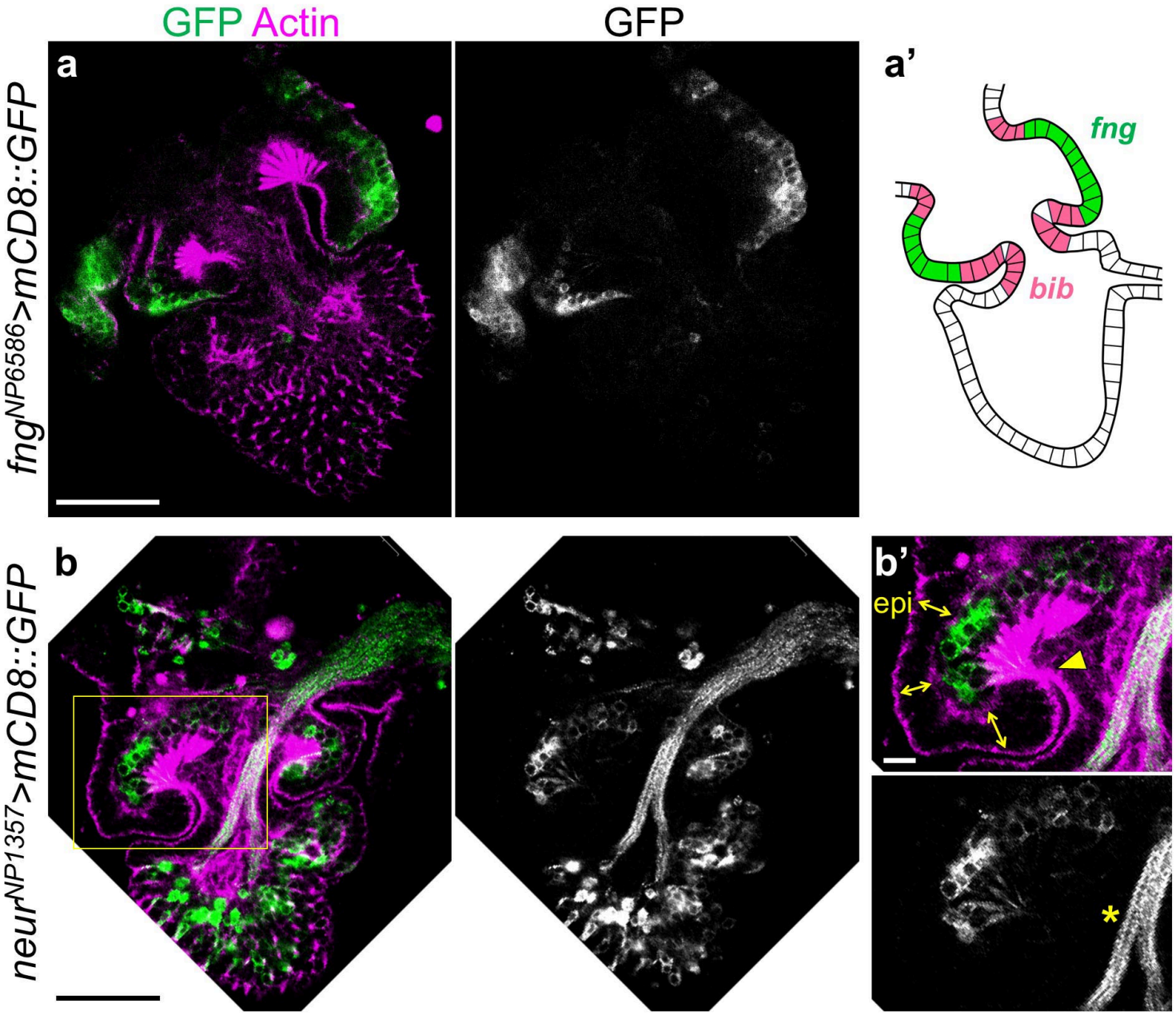


Figure 7

Expression of *fng*-GAL4 and *neur*-GAL4. **(a)** A representative antenna at 36-38 hours APF, in which the expression of a membrane-targeted GFP is driven by *fng*-GAL4 is stained for actin and viewed along the anterior-posterior axis. **(a')** A schematic drawing of *fng*-GAL4 expression in relation to *bib*-GAL4 expression. Whether the two drivers are expressed in an exactly complementary manner is not clear. **(b, b')** A representative antenna at 36-38 hours APF in which *neur*-GAL4 is used to express the membrane-targeted GFP, stained and viewed as in (a). A magnified view of the boxed region in (b) is shown in (b'). GFP is expressed in JO neurons, extending into the actin-rich scolopale and cap rods that are connected to the a2-a3 joint (arrowhead). GFP
expression is not detected in the epidermis (epi, double-headed arrows). Asterisk indicates axons extending from a3. (a) is flipped horizontally. Scale bars: 50 μm in (a, b), 10 μm in (b').

Supplementary Files

This is a list of supplementary files associated with this preprint. Click to download.

- JiangandTajiriSupplementary260611a.pdf